



Published in final edited form as:

J Biomed Mater Res A. 2021 August ; 109(8): 1512–1520. doi:10.1002/jbm.a.37142.

Interleukin-4 repairs wear particle induced osteolysis by modulating macrophage polarization and bone turnover

Jukka Pajarinen^{1,2,3}, Tzuhua Lin¹, Akira Nabeshima¹, Taishi Sato¹, Emmanuel Gibon¹, Eemeli Jämsen^{1,3}, Tahsin N. Khan¹, Zhenyu Yao¹, Stuart B. Goodman^{1,4}

¹Orthopaedic Research Laboratories, Department of Orthopaedic Surgery, Stanford University School of Medicine, Stanford, California ²Department of Musculoskeletal and Plastic Surgery, University of Helsinki and Helsinki University Hospital, Helsinki, Finland ³Department of Medicine, Clinicum, University of Helsinki and Helsinki University Hospital, Helsinki, Finland ⁴Department of Bioengineering, Stanford University, Stanford, California

Abstract

Periprosthetic osteolysis remains as a major complication of total joint replacement surgery. Modulation of macrophage polarization with interleukin-4 (IL-4) has emerged as an effective means to limit wear particle-induced osteolysis. The aim of this study was to evaluate the efficacy of local IL-4 delivery in treating preexisting particle-induced osteolysis. To this end, recently established 8 week modification of murine continuous femoral intramedullary particle infusion model was utilized. Subcutaneous infusion pumps were used to deliver polyethylene (PE) particles into mouse distal femur for 4 weeks to induce osteolysis. IL-4 was then added to the particle infusion for another 4 weeks. This delayed IL-4 treatment (IL-4 Del) was compared to IL-4 delivered continuously (IL-4 Cont) with PE particles from the beginning and to the infusion of particles alone for 8 weeks. Both IL-4 treatments were highly effective in preventing and repairing preexisting particle-induced bone loss as assessed by μ CT. Immunofluorescence indicated a significant reduction in the number of F4/80 + iNOS + M1 macrophages and increase in the number of F4/80 + CD206 + M2 macrophages with both IL-4 treatments. Reduction in the number of tartrate resistant acid phosphatase + osteoclasts and increase in the amount of alkaline phosphatase (ALP) + osteoblasts was also observed with both IL-4 treatments likely explaining the regeneration of bone in these samples. Interesting, slightly more bone formation and ALP + osteoblasts were seen in the IL-4 Del group than in the IL-4 Cont group although these differences were not statistically significant. The study is a proof of principle that osteolytic lesions can be repaired via modulation of macrophage polarization.

Keywords

interleukin-4; macrophage polarization; murine model; periprosthetic osteolysis; total joint replacement

1 | INTRODUCTION

Periprosthetic osteolysis and aseptic loosening remain as one of the leading causes for long-term failures and revision surgery of total joint replacements.¹ Periprosthetic osteolysis is mainly driven by ultra-high molecular weight polyethylene (UHMWPE) and other plastic and metal wear particles released from implant bearing surfaces and other implant interfaces.^{1,2} Wear particles are distributed to tissues surrounding the implant where they are phagocytosed by macrophages. Particle recognition and phagocytosis activate macrophages into an inflammatory phenotype leading to production of various chemokines and pro-inflammatory cytokines.^{3,4} Together these mediators trigger a chronic inflammatory reaction characterized by continued macrophage recruitment, increased osteoclastogenesis, and suppression of osteoblast function, ultimately leading to periprosthetic osteolytic lesions.^{4,5} Currently there are no means to mitigate the development of these lesions and the only treatment option available for advanced osteolysis is revision surgery. Since macrophages are the key cells mediating periprosthetic osteolysis, novel pharmacological treatment approaches targeting the particle-induced activation of macrophages has been a topic of intense research.

Macrophages are a dynamic population of cells that regulate both inflammation and tissue regeneration by sequentially assuming distinct functional phenotypes.^{6,7} The two polar extremes of this macrophage activation continuum are known as M1 and M2 macrophages: the former showing pro-inflammatory and antimicrobial characteristics and the latter having anti-inflammatory and tissue regenerative properties. Both macrophage phenotypes have been implicated in bone healing, with a brief period of M1 dominated inflammatory phase followed by an M2 tissue regenerative phase generally leading to optimal bone regeneration.^{8,9}

Biomaterial wear particles activate macrophages into an inflammatory, M1-like, phenotype characterized by continued production of pro-inflammatory cytokines and chemokines with detrimental effects on the surrounding bone.²⁻⁵ In contrast, induction of M2 macrophage polarization by interleukin-4 (IL-4) treatment mitigates wear particle-induced macrophage activation and inflammation in cell culture models.¹⁰⁻¹² Corresponding results were obtained using a mouse calvarial model in which local IL-4 injections significantly reduced acute UHMWPE particle-induced inflammation and osteolysis.¹³ Recently, the effects of IL-4 on more longstanding and chronic particle-induced osteolysis were studied in an established murine continuous femoral intramedullary particle infusion model.¹⁴ In this model, a delivery system consisting of a small osmotic pump, tubing, and a hollow titanium rod is used to continuously infuse UHMWPE particles into mouse distal femur during a course of 4 weeks.¹⁴⁻¹⁶ Using this model, IL-4 delivery together with UHMWPE particles effectively prevented inflammation-associated bone-loss.

These studies have demonstrated the potential of IL-4 in preventing the progression of particle-induced inflammation and osteolysis. However, the efficacy of IL-4 in treating osteolytic lesions that have already developed remains unclear. Indeed, considering the role that M2 macrophages play in bone regeneration, we hypothesized that induction of M2 polarization within the osteolytic lesions could be beneficial not only in preventing further

expansion of the lesion, but also to aid in its repair. Thus, the current study was designed to evaluate the efficacy of targeted IL-4 delivery in treating preexisting osteolytic lesions in a murine model that simulates the clinical scenario of developing peri-implant osteolysis. Using a recently established modification of a particle infusion model, local osteolysis was first introduced by delivering UHMWPE particles alone to the mouse distal femur continuously for 4 weeks.¹⁷ IL-4 was then added to the particle infusion by changing the subcutaneous pump in a minor surgery; the experiment was then continued for another 4 weeks with local delivery of both UHMWPE particles and IL-4 into the femur.^{17,18} This delayed IL-4 treatment (IL-4 Del) regimen was compared to IL-4 delivered continuously (IL-4 Cont) with polyethylene (PE) particles for 8 weeks and to infusion of particles alone. To assess the mechanisms of IL-4 action, the status of local macrophage polarization and cellular markers of bone turnover were studied. It was hypothesized that IL-4 delivery would modulate macrophage polarization toward M2 phenotype with potentially beneficial effects on bone regeneration.

2 | METHODS

2.1 | UHMWPE particles and osmotic pumps

Conventional UHMWPE particles were generated in total knee replacement simulator and isolated from the test supernatants following previously established protocol.^{16,17,19} Particles were then washed twice in ethanol (96 and 70%), resuspended in phosphate buffered saline (PBS), and stored in -80°C until used. Electron microscopy showed that most of the particles were spherical with a mean diameter of $0.48 \pm 0.10 \mu\text{m}$ (range $0.26\text{--}0.81 \mu\text{m}$). Particles did not contain a significant endotoxin contamination as tested with Limulus Amebocyte Lysate Kit (BioWhittaker, Walkersville, MD). Alzet osmotic pumps (Model 2006, Durect Corporation, Cupertino, CA) were loaded either with (a) carrier solution (1% BSA-PBS); (b) carrier solution with 15 mg/ml UHMWPE particles; or (c) carrier solution with UHMWPE particles and 10 $\mu\text{g/ml}$ mouse recombinant IL-4 (R&D Systems, Minneapolis, MN). Six-centimeter long vinyl tubing (Durect Corporation) was pre-filled with the appropriate solution, connected to the pumps, and subsequently used to connect the pumps to hollow A-40 titanium rods (6 mm long, 21 g, New England Small Tube, Litchfield, NH).

2.2 | Mouse model

The study was carried out in strict accordance to the National Academies' Guide for the Care and Use of Laboratory Animals along with institutional approval from the Administrative Panel on Laboratory Animal Care (APLAC) at Stanford University. A murine model of progressive wear particle-induced osteolysis was established as previously described.¹⁷ Forty-eight male BALB/cByJ mice (The Jackson Laboratory, Bar Harbor, ME) aged 10–12 weeks were first placed under isoflurane anesthesia. Using aseptic surgical technique right distal femur was exposed via lateral parapatellar arthrotomy and medial dislocation of the patella. An axial drill channel, extending from the intercondylar notch to the medullary cavity of the metaphyseal region, was created with a series of hypodermic needles. The hollow titanium rod was then press fit to the channel to an approximate depth of 3 mm. Osmotic pumps were then implanted in the subcutaneous tissue on the left-dorsal

side of the mouse and a subcutaneous tunnel reaching the right knee was created to connect the tubing to the implanted rods. Skin incisions were closed with 5–0 Ethicon sutures. In strict adherence to the institutional guidelines, the postoperative recovery of the mice was closely monitored and buprenorphine (0.1 mg/kg, SC, twice a day) given for postoperative analgesia. Mice were individually housed at Stanford animal housing facilities in a temperature-controlled environment on a 12 hr light–dark cycle with food and water being provided ad libitum. After 4 weeks, the mice were placed under isoflurane anesthesia and the pumps changed in a minor operation as previously described in detail.¹⁷ The experiment was continued for another 4 weeks (thus totaling 8 weeks of particle infusion), after which the mice were euthanized with CO₂ inhalation followed by cervical dislocation. Four experimental groups (n = 12 mice per group) were defined by the pump contents and the corresponding infusion as summarized in Table 1. The residual volume of both primary and secondary pumps was measured and compared to the theoretical infusion rate to confirm successful particle delivery.

2.3 | μ CT imaging

At 8 weeks after the initial surgery, femurs were collected, titanium rods carefully removed, and all femurs (n = 12) imaged with an explore Locus RS150 MicroCT scanner (GE Healthcare, Fairfield, CT). Scans were performed with 70 kVp, two frames per view, 360° rotation, 2 x 2 binning, and 49 μ m voxel size. Images were analyzed with GEMS MicroView software (GE Healthcare) with a 3 x 2.5 x 3 mm volume of interest drawn to the distal metaphyseal region using the epiphyseal plate as an anatomical landmark. Tissue mineral content (TMC) and bone volume fraction (BVF) were then determined using 700 HU as a threshold for bone tissue.

2.4 | Histological and immunohistochemical analyses

Following μ CT imaging the femurs were dissected free of soft tissues. Femurs were fixed in 4% paraformaldehyde for 1 day, decalcified in 0.5 M ethylenediaminetetraacetic acid (EDTA)-PBS for 2 weeks with decalcifying solution changed twice a week and embedded in OCT for sectioning. 8 μ m thick transverse plane frozen sections were cut from the distal metaphyseal region representing the end of the rod channel and the immediate area of particle delivery. Four representative mice per group were selected for the detailed histological analysis (n = 4).

Routine hematoxylin and eosins (H&E) stained sections were prepared and evaluated for general bone tissue morphology under Axio Observer 3.1 (Zeiss, Oberkochen, Germany) microscope.

The amount of osteoblast covered bone surfaces was determined with alkaline phosphatase (ALP) immunostaining. First, the tissue sections were fixed in ice-cold acetone for 10 min, followed by washing in PBS and blocking of endogenous peroxidase by 10 min treatment in Bloxall solution (Vector Laboratories, Burlingame, CA). Next, sections were washed in PBS and further blocked with 10% rabbit normal serum in 0.1% BSA-PBS for 1 hr. Normal serum was then decanted and polyclonal goat anti-mouse ALP antibody (AF2910, R&D systems) or corresponding negative control antibody (Goat IgG, Santa Cruz Biotechnology,

Santa Cruz CA), diluted to a final concentration of 5 µg/ml in 0.1% BSA-PBS, applied to the sections. After an overnight incubation at +4°C, the sections were thoroughly washed in PBS and incubated in biotinylated rabbit anti-goat secondary antibody (Vector Laboratories) diluted 1/200 in 0.1% BSA-PBS for 1 hr at room temperature. Sites of the biotinylated secondary antibody binding were visualized with Vectastain ABC kit and ImmPACT NovaRED peroxidase substrate kit (Both from Vector Laboratories) following manufacturer's instructions. Sections were counterstained with hematoxylin, dehydrated, and mounted with VectaMount (Vector Laboratories). Sections were imaged under Axio Observer 3.1. The percentage of bone surfaces covered either by cuboidal ALP + osteoblasts, flat ALP + bone lining cells or bone surface entirely devoid of ALP + cells was measured using ImageJ (National Institute of Health).

The number of osteoclasts was determined with tartrate resistant acid phosphatase (TRAP) histochemical staining kit (Sigma Aldrich, St. Louis, MO) following manufacturer's instructions. Osteoclasts were defined as multinucleated TRAP + cells located within resorption lacunae either in endosteal or trabecular bone surfaces and their total number per section was counted visually.

Total amount of macrophages at distal femur was determined by F4/80 immunofluorescence staining and the status of macrophage polarization assessed by F4/80 iNOS (for M1) and F4/80 CD206 (for M2) double immunofluorescence stainings with both the iNOS and CD206 (mannose receptor) being well characterized markers of M1 and M2 phenotype respectively.^{6,7} First, the tissue sections were fixed in ice cold acetone for 10 min, followed by washing in PBS, and blocking with 1% BSA-PBS for 1 hr in room temperature. Following blocking, monoclonal anti-mouse F4/80 AlexaFluor 647 conjugated antibody (MCA497A647, BioRad, Hercules, CA) or corresponding isotype control (BD Biosciences, San Jose, CA) was diluted 1% BSA-PBS to reach final concentration of 2 µg/ml and applied to tissue sections. For double immunofluorescence staining either Fluorescein isothiocyanate (FITC) conjugated monoclonal anti-mouse iNOS (4 µg/ml, 610331, BD Biosciences, San Jose, CA); phycoerythrin (PE) conjugated monoclonal anti-mouse CD206 antibody (1 µg/ml, 141706, Biolegend, San Diego, CA); or corresponding isotype controls were added to the F4/80 antibody dilutions at the indicated final concentrations and applied to the sections. After an overnight incubation in +4°C, sections were washed thoroughly in PBS, mounted with Pro-Long Gold with DAPI (Life Technologies) and imaged with Axio Observer 3.1. Total area of F4/80 positive cells, as well as the total area of F4/80 + iNOS+ and F4/80 + CD206+ double positive cells was quantified using ImageJ and normalized to the total area of cells observed in the image. The area quantification was done semi-automatically using standardized image thresholding, but each image was carefully assessed visually to ensure that the positive staining signal originated from the cells and not for example, from nonspecific background staining. If clearly nonspecific staining was observed, it was omitted from the quantification. A similar strategy was utilized to identify the double positive cells with only the double positive areas being included in the area quantification.

2.5 | Statistical analyses

Statistical analyses were conducted using GraphPad Prism version 6.03 (GraphPad Software, La Jolla, CA). ANOVA followed by Tukey's post-hoc tests was used for the statistical comparison of the experimental groups with $p < .05$ chosen as the threshold for significance. All values are presented as mean \pm SEM.

3 | RESULTS

3.1 | IL-4 treatments prevented and repaired particle induced bone loss assessed with μ CT

After 8 weeks of the implantation, a bony channel had formed around the titanium rods. This channel extended along the long axis of the femur, from the intercondylar notch to a metaphyseal region to a mean depth of 3 mm. In control samples, a dense network of metaphyseal trabecular bone surrounded the proximal end of the rod channel (Figure 1a). Continuous delivery of PE particles into the distal femur for 8 weeks resulted in local bone loss evident on μ CT analysis as significant reduction of both TMC and BVF compared to controls (Figure 1b). Both continuous and IL-4 Del prevented this particle induced bone loss. IL-4 Del group had the most bone at 8 weeks with both the TMC and BVF being significantly higher than in PE group and TMC significantly higher than in the continuous IL-4 treatment group. In the IL-4 continuous group TMC was significantly higher than in PE sample but the BVF did not reach statistical significance (Figure 1b). Qualitatively, particle treated samples showed thinner cortices and, in particular, evident loss of metaphyseal trabecular bone while both IL-4 treated groups showed bone microstructure similar to the control samples (Figure 1a).

3.2 | IL-4 treatments prevented particle induced osteoclast formation and supported osteoblast activity in histopathological analysis

Histological sections were obtained from the proximal end of the rod channel from the metaphyseal area most impacted by the particle and IL-4 delivery. Corresponding to the μ CT images, H&E stained samples showed formation of a bony interface around the end of the implant, surrounded by a network of trabecular bone and bone marrow. This architecture was particularly conspicuous in the control samples (Figure 2, panel 1a). In controls, endosteum and the surfaces of the bone trabecula were covered by cuboidal osteoblasts identified by ALP immunostaining, while osteoclasts identified with TRAP staining were scarce (Figure 2, panels 1b,c). In particle treated samples, a qualitative reduction in the amount of trabecular bone as well as a thinner bony interface around the implant was observed (Figure 2, panel 2a). This reduction in trabecular bone was accompanied by a significant reduction in the percentage of bone surface covered with either ALP + cuboidal osteoblasts or ALP + flat bone lining cells (Figure 2, panel 2b, left bar diagram). In contrast, the number of TRAP + osteoclasts per section was significantly increased by particle delivery, compared to the controls (Figure 2, panel 2c, right bar diagram). All of these adverse effects of the chronic particle exposure on bone were partially reversed by both IL-4 treatments (Figure 2, panels 3a–c and 4a–c, and bar diagrams). Qualitatively, the structure of the trabecular bone and interface tissue appeared similar to controls and the percentage of bone surface covered by ALP + osteoblasts or bone lining cells was partially restored.

Similarly, the number of TRAP⁺ osteoclasts was reduced to the level of controls by both of the IL-4 treatments.

3.3 | IL-4 treatments prevented particle induced M1 macrophage polarization and induced M2 polarization

A relatively low number of F4/80 positive macrophages were seen scattered around the peri-implant bone marrow in control samples (Figure 3, panel 1a). These macrophages were neither M1 nor M2 phenotype, as they did not express iNOS or CD206 after immunofluorescence double staining (Figure 3, panel 1b,c). With particle treatment, a significant increase in the number of F4/80 positive macrophages was observed in the bone marrow immediately adjacent to the rod and the rod outflow channel (Figure 3, panel 2a, left bar diagram). The vast majority of these cells were iNOS positive M1 macrophages, although also a statistically significant increase in CD206 positive M2 type macrophages was observed compared to the controls (Figure 3, panels 2b,c, middle and right bar diagram). Neither of the IL-4 treatments had an impact on the overall macrophage number that remained about the same as in the particle treated group (Figure 3, panels 3a, 4a, left bar diagram). However, the number of iNOS + M1 macrophages was significantly reduced by both of the IL-4 treatments (Figure 3 panels 3b, 4b, middle bar diagram). Most notably, a striking increase in the amount of CD206 macrophages was observed, with a large number of F4/80 + CD206⁺ double positive cells being scattered around the bone marrow in both of the IL-4 treated groups (Figure 3, panels 3c, 4c, right bar diagram).

4 | DISCUSSION

Modulation of macrophage polarization with IL-4 has emerged as a means to prevent wear particle induced inflammation and osteolysis.¹⁰⁻¹⁴ In this study, the efficacy of IL-4 treatment in repairing osteolytic lesions was assessed in a novel modification of a murine continuous femoral intramedullary particle infusion model. It has been previously comprehensively shown that in this model system, the osteolysis is present after 4 weeks of particle infusion and that, without intervention, the osteolysis progresses with continued particle delivery.¹⁴⁻¹⁷ Thus, local osteolysis was first established by intramedullary particle infusion for 4 weeks followed by targeted IL-4 delivery with particles for another 4 weeks. The successful delivery of biologically active IL-4 by this delivery system was also comprehensively validated in a prior study.¹⁸

As expected, the continued particle delivery resulted in evident local bone loss at 8 weeks with striking increase in the number of iNOS positive M1 macrophages. Wear particles activate macrophages both by increasing activation and expression of pattern recognition receptors such as toll-like receptors (TLRs) and, after particle phagocytosis, by causing damage to endosomal membranes leading to activation of the NLRP3 inflammasome.²⁰⁻²⁴ Activation of these danger-signaling pathways leads to production of various pro-inflammatory cytokines and chemokines, as well as upregulation of iNOS via STAT1 signaling. Pro-inflammatory cytokines such as TNF- α and IL-1 β directly stimulate osteoclasts and suppress osteoblasts thus linking the chronic inflammation to bone loss.³⁻⁵ The chronic inflammation also tilts the balance of RANKL/OPG production from local mesenchymal

cells to favor osteoclast formation.^{25,26} In addition, wear particles directly suppress Mesenchymal Stem Cell (MSC)-to-osteoblast differentiation as well as osteoblast function.²⁷ Indeed, in addition to the accumulation of M1 macrophages, increased numbers of osteoclasts and decreased number of osteoblasts were observed with continued particle delivery.

Both the continuous and IL-4 Dels were effective in not only preventing but also repairing particle induced bone loss. A reduction in the number of iNOS positive M1 macrophages and striking increase in the number of CD206 positive M2 macrophages was observed with both IL-4 treatment strategies. This change in the macrophage phenotype was accompanied by a reduction in the number of osteoclasts and restoration of osteoblast function. The main limitation of the study is that the exact molecular mechanisms by which IL-4 treatment resulted to these changes in the bone turnover were not investigated. The beneficial effects of IL-4 on repairing osteolysis could, however, have at least three potential explanations.

First, IL-4 has well documented anti-inflammatory and pro-regenerative effects on macrophages.^{6,7,28,29} By binding to its receptor on the cell membrane, IL-4 signals through the JAK-STAT6 pathway with many of the M2 polarization related genes such as CD206 and Arginase 1 being directly regulated by the transcription factor STAT6.^{28,29} IL-4 receptor also activates other intracellular signaling pathways leading to activation of transcription factor peroxisome proliferator-activated receptor- γ (PPAR γ). PPAR γ directly inhibits the activation of pro-inflammatory transcription factors such as NF- κ B that has been implicated in the macrophage's response against wear particles.²⁸⁻³⁰ Indeed, it has been comprehensively shown in cell culture models that IL-4 treatment prevents macrophages inflammatory response against wear particles.¹⁰⁻¹² The precise intracellular mechanisms of this IL-4 action are still to be elucidated but likely include suppression of pro-inflammatory signaling pathways and transcription factors. Of note, IL-4 also inhibits the activation of NLRP3 inflammasome and downregulates TLR expression potentially contributing to the suppression of wear particle induced inflammation.³¹⁻³³ Taken together, one potential mechanism by which IL-4 prevents and repairs particle induced osteolysis is by suppressing the particle induced macrophage activation thus blocking the adverse effects of inflammation on bone turnover. Interestingly, however, although IL-4 had clear impact on macrophage polarization, IL-4 did not impact macrophage recruitment as macrophage numbers between the IL-4 treated and nontreated samples remained similar.

Second, IL-4 has direct effects on both osteoclasts and osteoblasts. It has been comprehensively shown by studies spanning over three decades that IL-4 directly prevents osteoclast formation and function via STAT6 and PPAR γ mediated inhibition of NF- κ B.³⁴⁻³⁶ The effects of IL-4 on osteoblasts and MSC-to-osteoblast differentiation are less well understood. Cell culture studies on this matter are controversial as in some studies IL-4 prevents and, in some studies, enhances osteoblast differentiation and osteoblast mediated bone formation.³⁷⁻⁴¹ Furthermore, the effects of IL-4 on wear particle challenged MSCs or osteoblasts have not been studied to our knowledge. Direct in vivo evidence of IL-4 impact on bone formation is also scarce. IL-4 delivery has, however, been shown to enhance fracture repair and bone/implant integration thus providing indirect evidence of beneficial effect on bone formation in vivo.^{42,43} The current results provide further evidence that IL-4

treatment is indeed beneficial for osteoblast activity in vivo as clear restoration of osteoblast numbers and subsequent repair of osteolytic lesions was observed. Taken together, IL-4 has direct effects on both osteoclasts and osteoblasts that might partially explain the repair of the osteolytic lesions.

Last, an attractive possibility is that IL-4 enhances bone formation by favorably modulating the complex interactions between macrophages, osteoprogenitor cells, and osteoblasts. It is now increasingly understood that successful bone regeneration is based on the coordinated cross talk between these cell types.^{8,9,44} During fracture repair, macrophage-derived mediators such as Oncostatin M (OSM), Prostaglandin E2 (PGE-2), and Bone Morphogenetic Protein 2 (BMP-2) regulate the MSC-to-osteoblast differentiation with MSC reciprocally modulating macrophage activation.^{8,9,44} Evidence is emerging that timely modulation of macrophage polarization from M1 to M2 phenotype enhances bone formation by impacting the cross talk between these cell types.^{45,46} Indeed, in a wear particle challenged macrophage/MSC co-culture model, IL-4 enhanced bone formation and that this effect was associated to an increase in PGE-2 production.⁴⁷ It is tempting to speculate that the restoration of osteoblast function by IL-4 treatment was partly due to favorable modulation of macrophage/MSC cross talk.

The IL-4 Del strategy resulted to more bone at 8 weeks than the continuous IL-4 delivery. One possible explanation for the phenomenon is that modulation of macrophage phenotype too early during the repair of the initial surgical trauma could compromise the subsequent bone regeneration. Indeed, a period of inflammation followed by a pro-regenerative phase has been suggested to result in optimal bone healing.^{8,9,44} Alternatively, complete blockade of osteoclast function and inhibition of bone remodeling with extended IL-4 exposure could partially explain the observation.

The results are in line with previous in vitro studies showing that IL-4 is effective in preventing particle induced inflammation and bone loss.^{10-14,47} In addition, the results are a proof of principle that not only can the progression of osteolytic lesions be stopped but also partially repaired. Although still far from clinical applications, the results suggest that periprosthetic osteolysis could indeed be eventually managed by conservative means. While not necessarily curative, there are significant numbers of patients with osteolysis who are not good candidates for revision surgery, but who could benefit from partially repairing or even just slowing down the osteolytic process via a minimally invasive approach. The local delivery of IL-4 or similarly acting pharmaceutical agent could be achieved CT targeted injection and could potentially be repeated as needed. Alternatively, more elaborate means of drug delivery could be utilized. Indeed, a novel IL-4 delivery strategy based on genetically modified MSCs has recently been developed.^{48,49} These cells can deliver IL-4 either constitutively or in response to an inflammatory microenvironment allowing specific and on-demand IL-4 release. In cell culture model, these IL-4 releasing MSCs were effective in mitigating particle-induced inflammation and inducing bone formation.^{47,50} Although experimental, this approach is an example of an emerging, innovative strategy to limit particle-induced osteolysis by means of MSC cell therapy. The potential long-term effects of IL-4 are currently unknown and need to be thoroughly evaluated before clinical applications

as IL-4 has been suspected to contribute to the development of some tumors, although not to the extent that would currently prevent researching its therapeutic potential.⁵¹

In conclusion, both the continuous and IL-4 Dels were highly effective in preventing and even repairing preexisting particle induced inflammation and bone loss. Striking reduction in the number of M1 macrophages and increase in the number of M2 macrophages was observed with IL-4 treatment. We postulate that this switch in the macrophage phenotype with accompanied change in the cytokine microenvironment resulted in decreased osteoclast activity and increased osteoblast activity, ultimately resulting to the repair of bone in the IL-4 treated samples. The study is a proof of principle that osteolytic lesions can be repaired via modulation of macrophage polarization and suggest that periprosthetic osteolysis can eventually be managed by nonoperative means.

ACKNOWLEDGMENTS

This work was supported by NIH grants R01AR055650, R01AR063717, R01AR073145 and the Ellenburg Chair in Surgery at Stanford University. Jukka Pajarinen was supported by a grant from the Jane and Aatos Erkkö foundation. UHMWPE particles were a generous gift from Dr Timothy Wright (Hospital for Special Surgery). Imaging studies were conducted at Stanford Small Animal Imaging Service Center.

Funding information

Foundation for the National Institutes of Health, Grant/Award Numbers: R01AR055650, R01AR063717, R01AR073145; Jane ja Aatos Erkon Säätiö

DATA AVAILABILITY STATEMENT

Data available on request from the authors

REFERENCES

1. Pajarinen J, Lin TH, Sato T, Yao Z, Goodman S. Interaction of materials and biology in total joint replacement - successes, challenges and future directions. *J Mater Chem B Mater Biol Med*. 2014;2:7094–7108. [PubMed: 25541591]
2. Pajarinen J, Gallo J, Takagi M, Goodman SB, Mjöberg B. Particle disease really does exist. *Acta Orthop*. 2018;89:133–136. [PubMed: 29143557]
3. Ingham E, Fisher J. The role of macrophages in osteolysis of total joint replacement. *Biomaterials*. 2005;26:1271–1286. [PubMed: 15475057]
4. Nich C, Takakubo Y, Pajarinen J, et al. Macrophages-key cells in the response to wear debris from joint replacements. *J Biomed Mater Res A*. 2013;101:3033–3045. [PubMed: 23568608]
5. Landgraaber S, Jäger M, Jacobs JJ, Hallab NJ. The pathology of orthopedic implant failure is mediated by innate immune system cytokines. *Mediators Inflamm*. 2014;2014:1–9.
6. Mosser DM, Edwards JP. Exploring the full spectrum of macrophage activation. *Nat Rev Immunol*. 2008;8:958–969. [PubMed: 19029990]
7. Murray PJ, Wynn TA. Protective and pathogenic functions of macrophage subsets. *Nat Rev Immunol*. 2011;11:723–737. [PubMed: 21997792]
8. Claes L, Recknagel S, Ignatius A. Fracture healing under healthy and inflammatory conditions. *Nat Rev Rheumatol*. 2012;8:133–143. [PubMed: 22293759]
9. Pajarinen J, Lin T, Gibon E, et al. Mesenchymal stem cell-macrophage crosstalk and bone healing. *Biomaterials*. 2019;196:80–89. [PubMed: 29329642]
10. Rao AJ, Gibon E, Ma T, Yao Z, Smith RL, Goodman SB. Revision joint replacement, wear particles, and macrophage polarization. *Acta Biomater*. 2012;8:2815–2823. [PubMed: 22484696]

11. Pajarinen J, Kouri VP, Jämsen E, Li TF, Mandelin J, Konttinen YT. The response of macrophages to titanium particles is determined by macrophage polarization. *Acta Biomater.* 2013;9:9229–9240. [PubMed: 23827094]
12. Jämsen E, Pajarinen J, Lin TH, et al. Effect of aging on the macrophage response to titanium particles. *J Orthop Res in Press.* 2019;38: 405–416. 10.1002/jor.24461.
13. Rao AJ, Nich C, Dhulipala LS, et al. Local effect of IL-4 delivery on polyethylene particle induced osteolysis in the murine calvarium. *J Biomed Mater Res A.* 2013;101:1926–1934. [PubMed: 23225668]
14. Sato T, Pajarinen J, Behn A, et al. The effect of local IL-4 delivery or CCL2 blockade on implant fixation and bone structural properties in a mouse model of wear particle induced osteolysis. *J Biomed Mater Res A.* 2016;104:2255–2262. [PubMed: 27114284]
15. Ma T, Huang Z, Ren PG, et al. An in vivo murine model of continuous intramedullary infusion of polyethylene particles. *Biomaterials.* 2008; 29:3738–3742. [PubMed: 18561997]
16. Ren PG, Irani A, Huang Z, Ma T, Biswal S, Goodman SB. Continuous infusion of UHMWPE particles induces increased bone macrophages and osteolysis. *Clin Orthop Relat Res.* 2011;469:113–122. [PubMed: 21042895]
17. Pajarinen J, Nabeshima A, Lin TH, et al. Murine model of progressive orthopedic wear particle-induced chronic inflammation and osteolysis. *Tissue Eng Part C Methods.* 2017;23:1003–1011. [PubMed: 28978284]
18. Pajarinen J, Tamaki Y, Antonios JK, et al. Modulation of mouse macrophage polarization in vitro using IL-4 delivery by osmotic pumps. *J Biomed Mater Res A.* 2015;103:1339–1345. [PubMed: 25044942]
19. Gibon E, Ma T, Ren PG, et al. Selective inhibition of the MCP-1-CCR2 ligand-receptor axis decreases systemic trafficking of macrophages in the presence of UHMWPE particles. *J Orthop Res.* 2012;30:547–553. [PubMed: 21913218]
20. Caicedo MS, Desai R, McAllister K, Reddy A, Jacobs JJ, Hallab NJ. Soluble and particulate Co-Cr-Mo alloy implant metals activate the inflammasome danger signaling pathway in human macrophages: a novel mechanism for implant debris reactivity. *J Orthop Res.* 2009;27:847–854. [PubMed: 19105226]
21. Pearl JI, Ma T, Irani AR, et al. Role of the toll-like receptor pathway in the recognition of orthopedic implant wear-debris particles. *Biomaterials.* 2011;32:5535–5542. [PubMed: 21592562]
22. Burton L, Paget D, Binder NB, et al. Orthopedic wear debris mediated inflammatory osteolysis is mediated in part by NALP3 inflammasome activation. *J Orthop Res.* 2013;31:73–80. [PubMed: 22933241]
23. Caicedo MS, Samelko L, McAllister K, Jacobs JJ, Hallab NJ. Increasing both CoCrMo-alloy particle size and surface irregularity induces increased macrophage inflammasome activation in vitro potentially through lysosomal destabilization mechanisms. *J Orthop Res.* 2013; 31:1633–1642. [PubMed: 23794526]
24. Manzano GW, Fort BP, Dubyak GR, Greenfield EM. Wear particle-induced priming of the NLRP3 inflammasome depends on adherent pathogen-associated molecular patterns and their cognate toll-like receptors: an in vitro study. *Clin Orthop Relat Res.* 2018;476:2442–2453. [PubMed: 30427314]
25. Mandelin J, Li TF, Hukkanen M, et al. Interface tissue fibroblasts from loose total hip replacement prosthesis produce receptor activator of nuclear factor-kappaB ligand, osteoprotegerin, and cathepsin K. *J Rheumatol.* 2005;32:713–720. [PubMed: 15801030]
26. Mandelin J, Liljeström M, Li TF, et al. Pseudosynovial fluid from loosened total hip prosthesis induces osteoclast formation. *J Biomed Mater Res B Appl Biomater.* 2005;74:582–588. [PubMed: 15768436]
27. Pajarinen J, Lin TH, Nabeshima A, et al. Mesenchymal stem cells in the aseptic loosening of total joint replacements. *J Biomed Mater Res A.* 2017;105:1195–1207. [PubMed: 27977880]
28. Lawrence T, Natoli G. Transcriptional regulation of macrophage polarization: enabling diversity with identity. *Nat Rev Immunol.* 2011;11: 750–761. [PubMed: 22025054]

29. Galli SJ, Borregaard N, Wynn TA. Phenotypic and functional plasticity of cells of innate immunity: macrophages, mast cells and neutrophils. *Nat Immunol*. 2011;12:1035–1104. [PubMed: 22012443]
30. Lin TH, Pajarinen J, Lu L, et al. NF- κ B as a therapeutic target in inflammatory-associated bone diseases. *Adv Protein Chem Struct Biol*. 2017;107:117–154. [PubMed: 28215222]
31. Staeger H, Schaffner A, Schneemann M. Human toll-like receptors 2 and 4 are targets for deactivation of mononuclear phagocytes by interleukin-4. *Immunol Lett*. 2000;71:1–3. [PubMed: 10709778]
32. Ahn S, Jeong D, Oh SJ, Ahn J, Lee SH, Chung DH. GM-CSF and IL-4 produced by NKT cells inversely regulate IL-1 β production by macrophages. *Immunol Lett*. 2017;182:50–56. [PubMed: 28063891]
33. Awad F, Assrawi E, Jumeau C, et al. Impact of human monocyte and macrophage polarization on NLR expression and NLRP3 inflammasome activation. *PLoS ONE*. 2017;12:e0175336. [PubMed: 28403163]
34. Abu-Amer Y IL-4 abrogates osteoclastogenesis through STAT6-dependent inhibition of NF-kappaB. *J Clin Invest*. 2001;107: 1375–1385. [PubMed: 11390419]
35. Bendixen AC, Shevde NK, Dienger KM, Willson TM, Funk CD, Pike JW. IL-4 inhibits osteoclast formation through a direct action on osteoclast precursors via peroxisome proliferator-activated receptor gamma 1. *Proc Natl Acad Sci U S A*. 2001;98:2443–2448. [PubMed: 11226258]
36. Wei S, Wang MW, Teitelbaum SL, Ross FP. Interleukin-4 reversibly inhibits osteoclastogenesis via inhibition of NF-kappa B and mitogen-activated protein kinase signaling. *J Biol Chem*. 2002;277: 6622–6630. [PubMed: 11719504]
37. Ueno K, Katayama T, Miyamoto T, Koshihara Y. Interleukin-4 enhances in vitro mineralization in human osteoblast-like cells. *Biochem Biophys Res Commun*. 1992;189:1521–1526. [PubMed: 1282804]
38. Riancho JA, González-Marcías J, Amado JA, Olmos JM, Fernández-Luna JL, CJI S. Interleukin-4 as a bone regulatory factor: effects on murine osteoblast-like cells. *J Endocrinol Invest*. 1995;18:174–179. [PubMed: 7542294]
39. Ura K, Morimoto I, Watanabe K, Saito K, Yanagihara N, Eto S. Interleukin (IL)-4 and IL-13 inhibit the differentiation of murine osteoblastic MC3T3-E1 cells. *Endocr J*. 2000;47:293–302. [PubMed: 11036873]
40. Frost A, Jonsson KB, Brändström H, Ljunghall S, Nilsson O, Ljunggren O. Interleukin (IL)-13 and IL-4 inhibit proliferation and stimulate IL-6 formation in human osteoblasts: evidence for involvement of receptor subunits IL-13R, IL-13Ralpha, and IL-4Ralpha. *Bone*. 2001;28:268–274. [PubMed: 11248656]
41. Penno H, Frost A, Nilsson O, Ljunggren O. Expression of markers of activity in cultured human osteoblasts: effects of interleukin-4 and interleukin-13. *Scand J Clin Lab Invest*. 2010;70:338–342. [PubMed: 20509757]
42. Schlundt C, El Khassawna T, Serra A, et al. Macrophages in bone fracture healing: their essential role in endochondral ossification. *Bone*. 2018;106:78–89. [PubMed: 26529389]
43. Hachim D, LoPresti ST, Yates CC, Brown BN. Shifts in macrophage phenotype at the biomaterial interface via IL-4 eluting coatings are associated with improved implant integration. *Biomaterials*. 2017;112: 95–107. [PubMed: 27760399]
44. Loi F, Córdova LA, Pajarinen J, Lin TH, Yao Z, Goodman SB. Inflammation, fracture and bone repair. *Bone*. 2016;86:119–130. [PubMed: 26946132]
45. Loi F, Córdova LA, Zhang R, et al. The effects of immunomodulation by macrophage subsets on osteogenesis in vitro. *Stem Cell Res Ther*. 2016;7:15. [PubMed: 26801095]
46. Nathan K, Lu LY, Lin T, et al. Precise immunomodulation of the M1 to M2 macrophage transition enhances mesenchymal stem cell osteogenesis and differs by sex. *Bone Joint Res*. 2019;8:481–488. [PubMed: 31728188]
47. Lin T, Kohno Y, Huang JF, et al. Preconditioned or IL4-secreting mesenchymal stem cells enhanced osteogenesis at different stages. *Tissue Eng Part A*. 2019;25:1096–1103. [PubMed: 30652628]

48. Lin T, Pajarinen J, Nabeshima A, et al. Establishment of NF- κ B sensing and interleukin-4 secreting mesenchymal stromal cells as an “on-demand” drug delivery system to modulate inflammation. *Cytotherapy*. 2017;19:1025–1034. [PubMed: 28739167]
49. Lin T, Pajarinen J, Kohno Y, et al. Transplanted interleukin-4-secreting mesenchymal stromal cells show extended survival and increased bone mineral density in the murine femur. *Cytotherapy*. 2018;20:1028–1036. [PubMed: 30077567]
50. Lin T, Kohno Y, Huang JF, et al. NF κ B sensing IL-4 secreting mesenchymal stem cells mitigate the proinflammatory response of macrophages exposed to polyethylene wear particles. *J Biomed Mater Res A*. 2018;106:2744–2752. [PubMed: 30084534]
51. Setrerrahmane S, Xu H. Tumor-related interleukins: old validated targets for new anti-cancer drug development. *Mol Cancer*. 2017;16:153. [PubMed: 28927416]

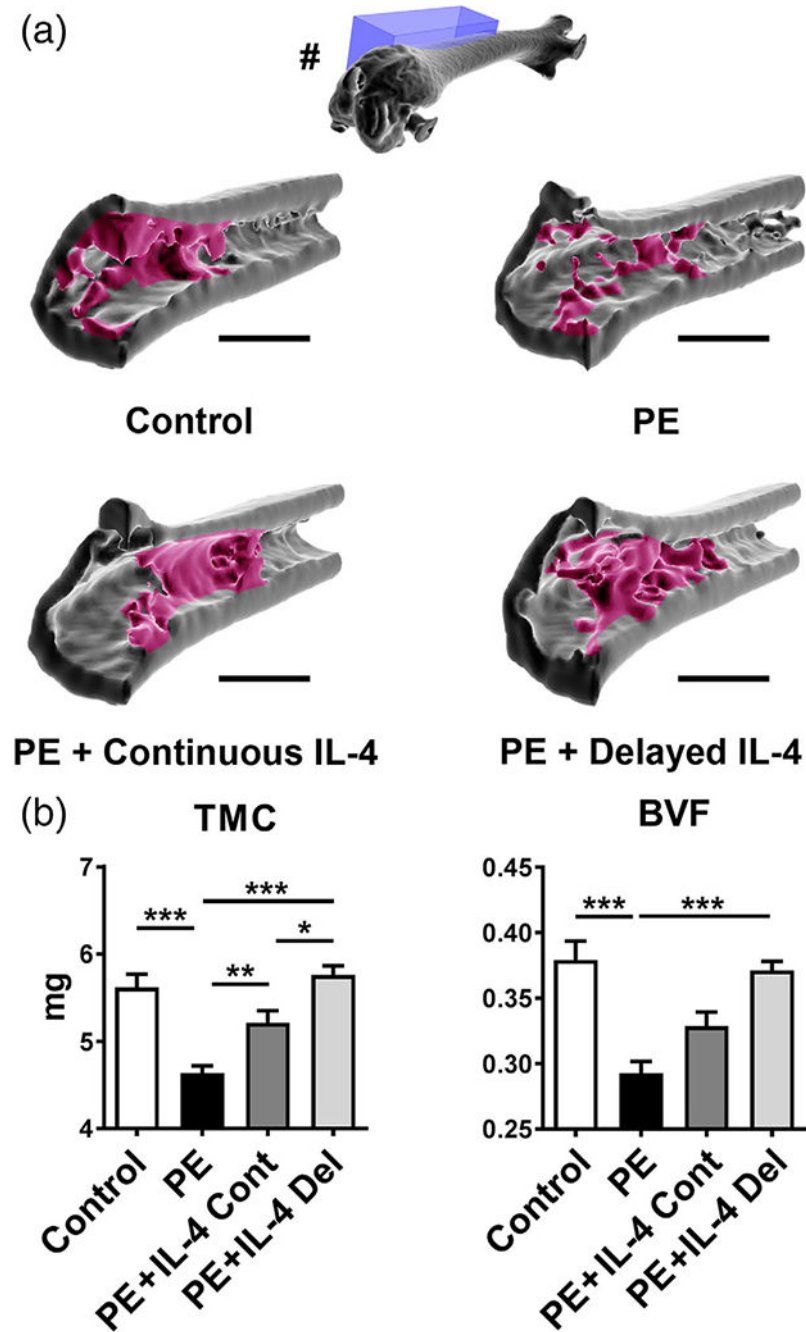


FIGURE 1.

The effects of IL-4 delivery on the particle-induced osteolysis as assessed by μ CT. Polyethylene (PE) particles were delivered into the mouse distal femur for 8 weeks through hollow titanium rod. IL-4 was added to the particle infusion either from the beginning of the particle delivery (IL-4 continuous, IL-4 Cont) or after 4 weeks (IL-4 delayed, IL-4 Del). At 8 weeks, the amount of bone at the distal femur was determined by μ CT imaging. (a) 3D reconstructions of a sagittal segment of distal metaphyseal region of the femur. Note the loss of metaphyseal and peri-implant trabecular bone in the PE infused samples and the

restoration of bone in the IL-4 treated samples. In the 3D reconstruction of the whole femur (#) the location of the sagittal 3D reconstructions (blue box) is shown. Notice also the rod channel visible in the intercondylar region of the whole femur reconstruction. (b) Bar diagrams showing the tissue mineral content (TMC) and bone volume fraction (BVF) at the distal femur. n = 12 mice per group. * = $p < .05$, ** = $p < .01$ *** = $p < .001$. Main regions of metaphyseal trabecular bone are indicated with red. Scale bars 1,500 μm

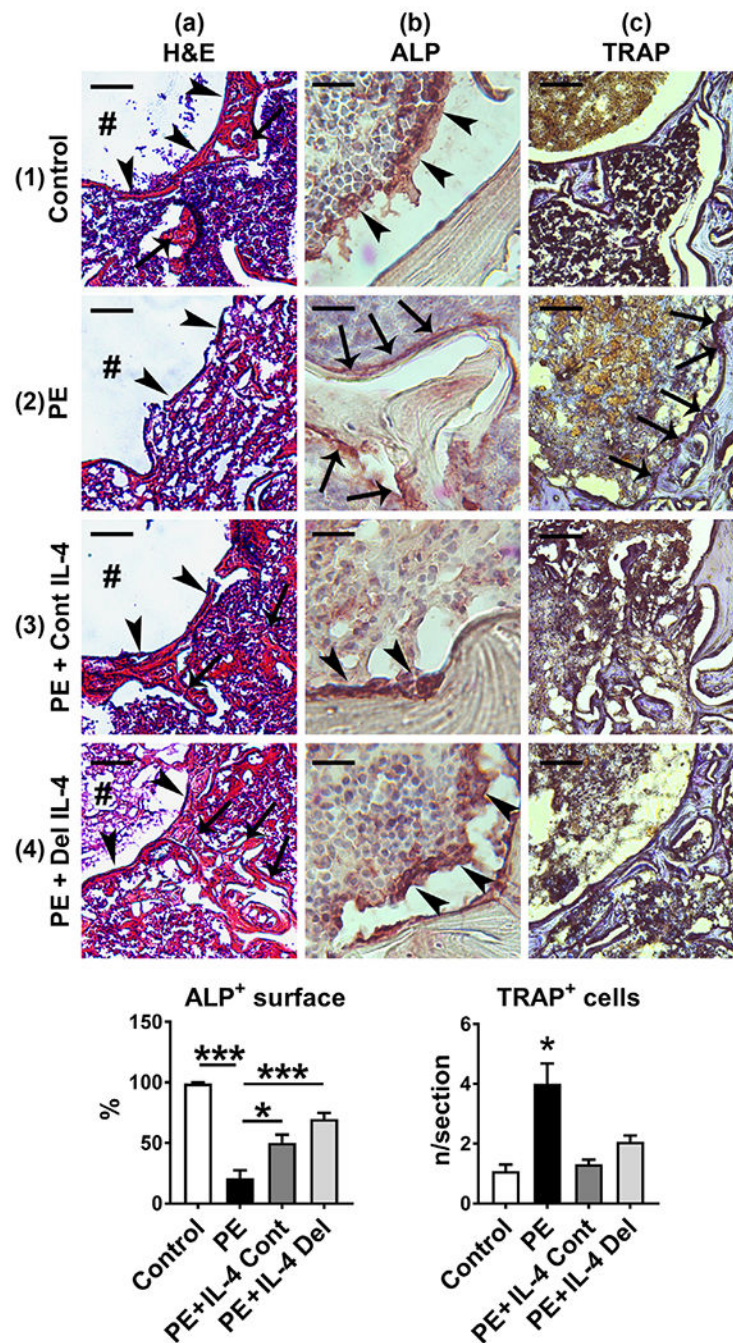


FIGURE 2.

The effects of IL-4 delivery on the bone microstructure and the amount of osteoclasts and osteoblasts. Polyethylene (PE) particles were delivered into the mouse distal femur for 8 weeks through hollow titanium rod. IL-4 was added to the particle infusion either from the beginning of the particle delivery (IL-4 continuous, IL-4 Cont) or after 4 weeks (IL-4 delayed, IL-4 Del). At 8 weeks, the overall tissue morphology at the distal femur was evaluated from hematoxylin and eosins (H&E) stained transverse tissue sections (panels 1–4a). In the control sample note the formation of a bony interface (arrowheads) around the

end of the implant channel (#), surrounded by a network of trabecular bone (arrows) and bone marrow (panel 1a). Note also the loss of bony interface (arrowheads) and the surrounding trabecular bone in the PE treated sample (panel 2a) and the marked restoration of these bone structures in the IL-4 infused samples (panels 3–4a, arrowheads and arrows). The amount of osteoblasts was determined by ALP immunostaining (Panels 1-4b the left bar diagram, * = $p < .05$, *** = $p < .001$). Note the large cuboidal osteoblasts (brown staining cells, arrowheads) covering the endosteal surfaces of the bone trabecula in the control and in the IL-4 treated samples. In contrast, in the PE sample endosteum was either devoid of ALP positive cells or covered by flat inactive appearing bone lining cells (arrows). The amount of osteoclasts was determined by TRAP histochemistry (panels 1–4c and right bar diagram, * = $p < 0.05$ PE vs. all other groups). Note the increase in the amount of osteoclasts and the marked erosion of the bone in the PE sample (purple staining cells, arrows) and the reduction of the osteoclast number by both of the IL-4 treatments. $n = 4$ mice per group. Scale bars in the panels 1–4a 100 μm ; Panels 1–4b 20 μm ; Panels 1–4c 50 μm . ALP, alkaline phosphatase; TRAP, tartrate resistant acid phosphatase

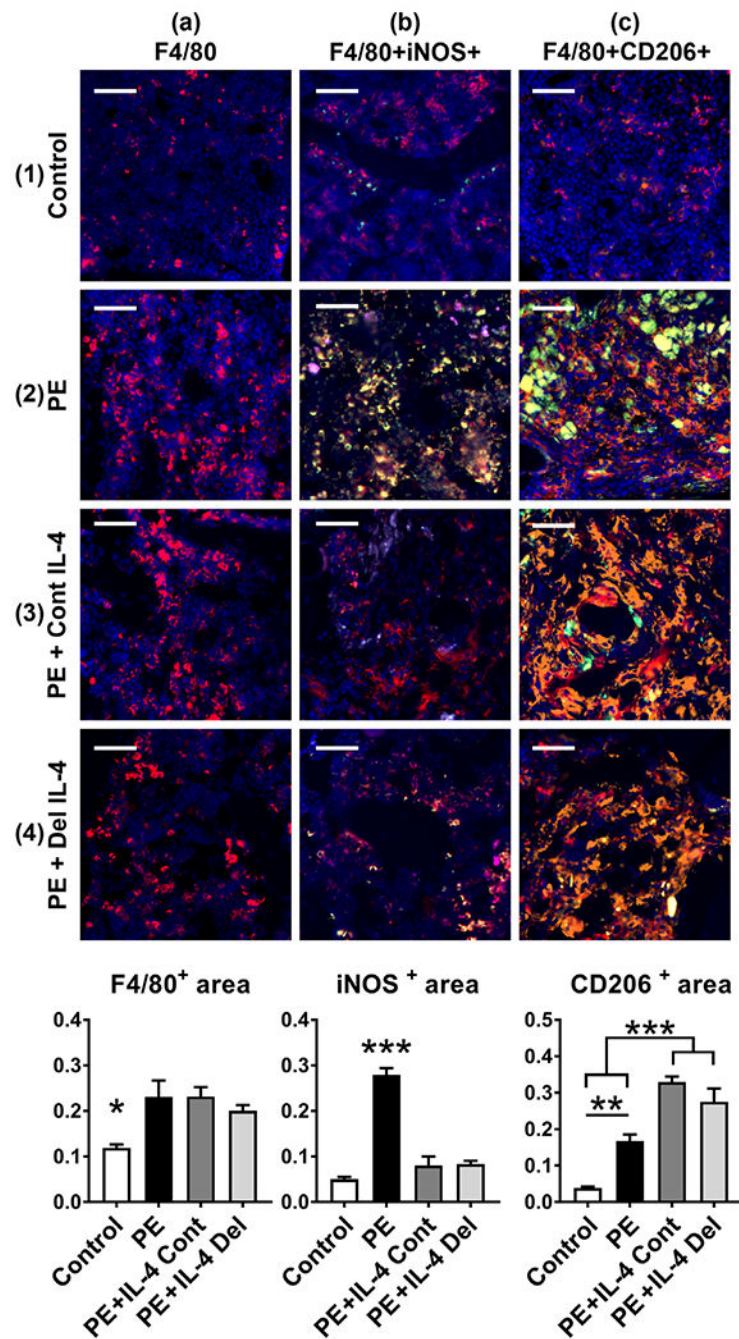


FIGURE 3.

The effects of IL-4 delivery on the macrophage polarization. Polyethylene (PE) particles were delivered into the mouse distal femur for 8 weeks through hollow titanium rod. IL-4 was added to the particle infusion either from the beginning of the particle delivery (IL-4 continuous, IL-4 Cont) or after 4 weeks (IL-4 delayed, IL-4 Del). At 8 weeks, the amount of macrophages at the distal femur was determined by F4/80 immunofluorescence staining (panels 1–4a, left bar diagram, * = $p < .05$ control vs. all other groups). Notice the increase in the amount of F4/80 positive macrophages in the metaphyseal bone marrow with the PE

treatment. The amount of M1 macrophages was determined by F4/80 iNOS immunofluorescence double staining (panels 1–4b, middle bar diagram, *** = $p < .001$ PE vs. all other groups). Notice the increase of F4/80 + iNOS double positive M1 macrophages in the PE sample and the reduction in the amount of M1 macrophages by both of the IL-4 treatments. The amount of M2 macrophages was determined by F4/80 CD206 immunofluorescence double staining (panels 1–4c, right bar diagram, ** = $p < .01$ *** = $p < .001$). Notice the increase of F4/80 + CD206 double positive M2 macrophages by both of the IL-4 treatments. A modest increase in the M2 macrophages was observed also in the PE samples. F4/80—red; iNOS—green; CD206—orange; DAPI—blue. The large green bodies visible in some of the pictures are polyethylene particle aggregates. $n = 4$ mice per group. Scale bars 50 μm

TABLE 1

The experimental groups. A subcutaneously implanted infusion pump was used to deliver polyethylene (PE) particles into the mouse distal femur. After 4 weeks, the pump was changed in a minor surgery and the experiment continued for another 4 weeks. IL-4 was added to the particle infusion either from the beginning of the particle delivery (IL-4 continuous) or after 4 weeks (IL-4 delayed) at which point local osteolysis had already been established. Pump contents for each experimental group are shown for clarity

Group	Pump contents	
	Weeks 1–4	Weeks 5–8
Control	Carrier	Carrier
PE	PE	PE
IL-4 continuous	PE + IL-4	PE + IL-4
IL-4 delayed	PE	PE + IL-4

Abbreviations: IL-4, interleukin-4; PE, polyethylene.